

1 Dynamical Cross-Correlated Physics Project

– Quantum-beam studies on dynamical cross-correlated physics in strongly-correlated-electron systems –

Project Leader: Hajime Sagayama

Charge, spin, orbital occupancy, orbital angular momentum, and the lattice system constitute degrees of freedom and dominate physical phenomena in materials. When more than one of them simultaneously act (multiferroicity), cross-correlation allows to express non-conjugated external field responses such as magnetization change by applying an electric field or electric polarization change by applying a magnetic field, producing advanced features in a monolithic device. Actually, electric and magnetic field responses of lattice distortion have already been put into practical use as piezoelectric and magnetostrictive devices, respectively. Compared to these, the correlation between magnetism and ferroelectricity has been considered to be difficult to exploit as a device in practical scenarios because of its weakness.

The objective of this project is to clarify the underlying mechanism of the notable cross-correlation properties of strongly electron correlated materials from a microscopic point of view. Stud-

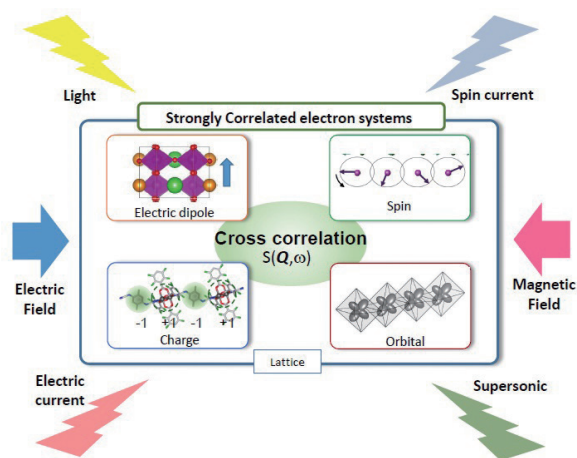


Fig. 1: Schematic view of cross-correlation for multi-degree of freedom in terms of spin, electric polarization, charge, orbital, and lattice in strongly correlated electron systems.

ies in progress are listed next:

1. Competition between antiferroelectricity and charge density wave (CDW) in layered BiS_2 -based superconductor.
2. Observation of critical electromagnetic fluctuations in the multiferroic material MnWO_4 .
3. Microscopic mechanism of large dynamical and static electromagnetic response in $\text{Co}_4\text{Nb}_2\text{O}_9$.
4. Electronic polarization induced by orbital ordering in A-site ordered perovskite manganites.

In this document, only the first study is described because of space limitation.

BiS_2 -based superconductors such as $\text{RO}_{1-x}\text{FxBiS}_2$ (where R denotes rare-earth ions) exhibit a layered structure that is analogous to the high- T_C cuprate and Fe-based superconductors [1-3]. They crystallize in a tetragonal structure with the space group $P4/nmm$, where double BiS_2 layers and RO block layers alternately stack along the c -axis (see Fig. 2). The mother material ROBiS_2 is a band insulator or semi-metal. By partial substitution of divalent oxygen ions for univalent fluorine ions, it becomes metallic, giving rise to superconductivity. Several first-principle calculations indicate that the F substitution generates electron carriers in a two-dimensional conduction band, which consists of Bi-6p and in-plane S-3p electron orbitals [4]. The substitution enhances T_C , which is maximized around $x \sim 0.5$ [5-8]. The value of T_C further increases under hydrostatic pressure [9-12]. A superconductive pairing mechanism of $\text{RO}_{1-x}\text{FxBiS}_2$ is still under debate. Unconventional superconductive states such as extended s-, p-, d-, and g-wave pairings, and weak topological superconductivity have been proposed.

In this study, we focus on $R = \text{La}$, where

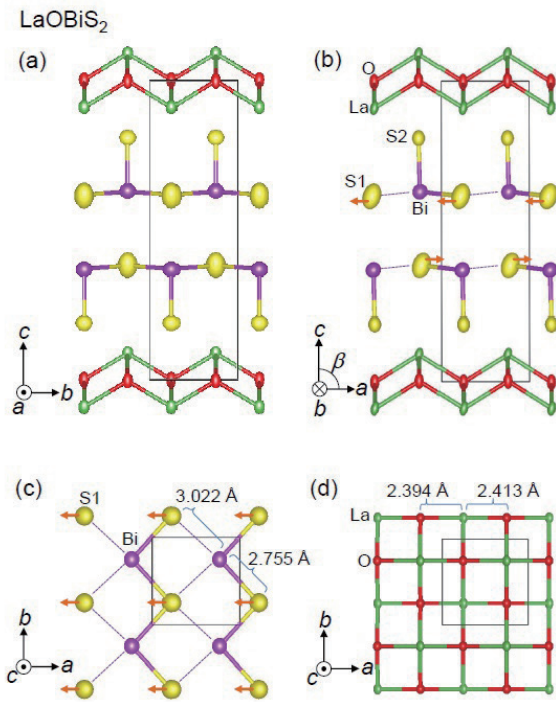


Fig. 2: Crystal structure of LaOBiS_2 projected along the (a) a -axis and (b) b -axis; (c) BiS_2 layer projected along the c -axis; (d) LaO block layer projected along the c -axis. Each ion is shown with anisotropic thermal ellipsoids at room temperature. These are sited according to [13].

the value of T_c is the highest among BiS_2 -based layered superconductors. For $x = 0.5$ ($\text{LaO}_{0.5}\text{F}_{0.5}\text{BiS}_2$), T_c is 2.6 K at ambient pressure and jumps up to 10.7 K under pressure at 0.5 GPa. Associated with this jump, the crystal structure changes from tetragonal system to the monoclinic system with space group $P2_1/m$.

Firstly, we investigated the crystal structure of the mother material LaOBiS_2 at room temperature under ambient pressure [13]. X-ray diffraction measurements were performed at Photon Factory (PF) and Photon Factory Advanced Ring (PF-AR), High Energy Accelerator Research Organization (KEK). Splitting of the fundamental reflections indicates monoclinic lattice distortion. The space group was determined as $P2_1/m$, which is identical to the leading candidate in the HP phase [12]. Figure 2 depicts the crystal structure of LaOBiS_2 projected along the a -, b -, and c -axes. It is noticeable that the S1 ions uniformly shift along the a -axis, whereas the deformation of the LaO block is negligible [Figs. 2(c) and 3(d)]. Given that the directions of the shift are opposite in the two adjacent BiS_2 layers (antiferroelectricity), the spatial inversion symmetry remains at the midpoint of these two BiS_2 layers. The lattice distortion origi-

nates from lattice instability owing to size mismatch between LaO blocks and BiS_2 sheets, in turn caused by the fact that the ionic size of the La is the largest among those of the rare-earth ions [14].

Since lattice deformation of the Bi-S1 plane would affect the Fermi surface, structural change due to the F substitution should be investigated as well as its electronic state to understand the pairing mechanism. We also investigated the lattice structure of $\text{LaO}_{0.5}\text{F}_{0.5}\text{BiS}_2$ on single crystal samples [15]. The space group is kept to be $P4/nmm$ at room temperature. The thermal ellipsoid of S1 is more than twice as large as other ions and almost isotropic, suggesting large instability of S1. Then, we investigated the structural change in temperature down to 30 K. All fundamental reflections exhibit no splitting, indicating that the space group of the mean structure remains a tetragonal system at low temperature. Remarkably, super-lattice reflections with propagation vector $q = (\zeta \zeta 1/2)$ was newly found, where $\zeta \sim 0.207$ below $T^* \sim 260$ K. Profiles of the fundamental reflections $(4\ 0\ 0)$ and the satellite reflections $(4-\zeta-\zeta\ 0.5)$ at various temperatures are shown in Fig. 3 (a). Integrated intensity of the $(4-\zeta-\zeta\ 0.5)$

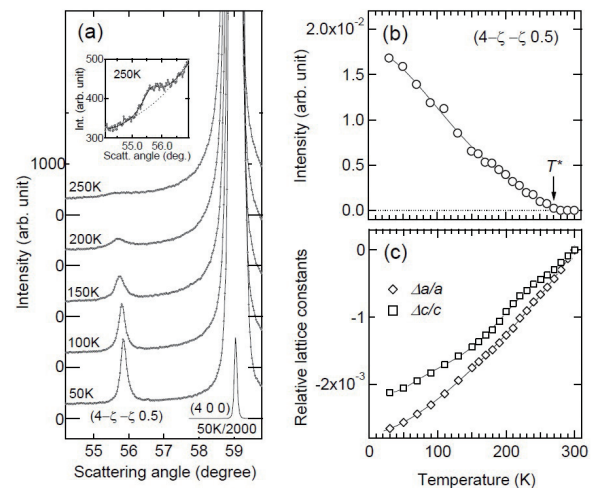


Fig. 3: (a) X-ray diffraction profiles of $(4\ 0\ 0)$ and $(4-\zeta-\zeta\ 0.5)$ reflections of $\text{LaO}_{0.5}\text{F}_{0.5}\text{BiS}_2$ observed at 250 K, 200 K, 150 K, 100 K, and 50 K. Black solid line represents the profile of the $(4\ 0\ 0)$ reflection over two thousand reflections observed at 50 K. Insets illustrate the enlarged view of $(4-\zeta-\zeta\ 0.5)$ reflection profiles observed at 250 K.; (b) Temperature variation of the integrated intensity of $(4-\zeta-\zeta\ 0.5)$ reflection; (c) Temperature variation of the relative lattice constants, a and c . These are cited from [15].

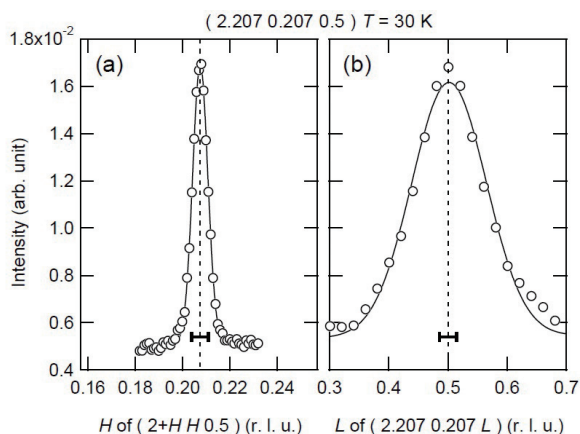


Fig. 4: Profiles of the $(2-\zeta \zeta 0.5)$ reflection scanned along the $(H H 0)$ direction (a) and the $(0 0 L)$ direction (b) in the reciprocal space [15]. The experimental resolutions denoted by the bold horizontal lines are derived from the $(2 0 0)$ reflection profiles.

gradually increases with decreasing temperature. In particular, temperature dependences of lattice constants a and c are shown in Fig. 3(c), in which noticeable anomalous behavior is not found around T^* . These results highlight the second or higher order transition at T^* . Width of the satellite reflection is three times as large as that of the $(4 0 0)$ reflection even at 30 K, suggesting spatial short-range modulation. To determine the correlation length of the super-lattice structure, we examined the profile of the $(2-\zeta \zeta 0.5)$ reflection along $(H H 0)$ and $(0 0 L)$ directions in the reciprocal space. As depicted in Fig. 4, the peak width of $(0 0 L)$ scan is quite larger than the experimental resolution, while that of the $(H H 0)$ scan is comparable to its resolution. Correlation lengths along the c -axis are estimated to be $6.9c$ ($\sim 92 \text{ \AA}$), indicating that interlayer interaction is relatively weak.

The existence of the super-lattice structure would affect conduction electron band and lattice instability. For instance, CDW will open a gap on the Fermi surface that commonly leads to suppress superconductivity. For clarifying the interplay between the super-lattice structure and superconductivity, we investigated the pressure change of the observed super-lattice reflections. Fig. 5 shows x-ray oscillation photographs taken at ambient pressure (a) and at 1.2 GPa (b), where high- T_C phase is induced. At ambient pressure, $(2 0 0)$ reflection and its satellite super-lattice reflections can be clearly observed. At 1.2 GPa, the super-lattice reflections disappear, while $(1 0 0)$ and $(2 1 0)$ reflections appear instead. Both reflections

are absent at ambient pressure because of the extinction rule of $P4/nmm$. Existence of these reflections at 1.2 GPa demonstrates the monoclinic structure with space group $P2_1/m$ in the high- T_C phase.

Here we consider the super-lattice structure from a microscopic point of view. A number of theoretical studies predicted the strong nesting condition on rectangular Fermi surfaces [4]. It could give rise to CDW state with lattice modulation of BiS sheets. Actually, lattice instability at the M point is theoretically predicted [14, 16]. In these theoretical studies, the L component of the expected propagation vector is 0, probably because this material is assumed to be a two-dimensional system. However, the obtained propagation vector is $\zeta \zeta 0.5$, indicating that the interlayer interaction is weak but should not be ignored when it comes to analyzing lattice instability and electronic state. Phonon dispersion relations calculated by Li only predict obvious softening between Z $(0 0 0.5)$ and R $(0.5 0.5 0.5)$ [35]. Lattice modulation with the propagation vector $(\zeta \zeta 0.5)$ could be stabilized by freezing it. Given that the origin of the softening has not been well established, further investigation is strongly expected.

The super-lattice reflections disappear accompanied by the pressure-induced structural phase transition, as depicted in Fig. 5. This result suggests the competitive relation between the static super-lattice structure and the superconductivity in $\text{LaO}_{0.5}\text{F}_{0.5}\text{BiS}_2$. The super structure must be taken into account for consideration of electronic state and lattice dynamics. Assuming that T_C is

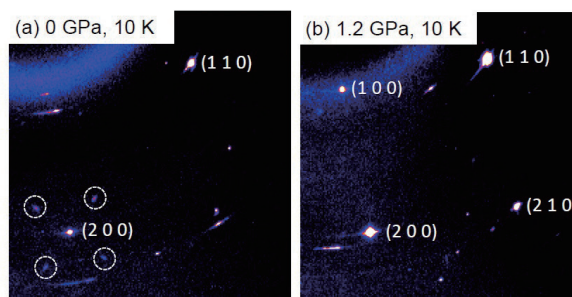


Fig. 5: Representative examples of X-ray oscillation photographs observed under ambient pressure at 10 K (a) and at 1.2 GPa and 10 K (b) [15]. The dashed circles denote super-lattice reflections with propagation vectors $(\zeta \zeta 0.5)$. The unassigned spots might be scattering from NaCl, Be metal, or gasket.

suppressed by the super-lattice structure at ambient pressure, pressure-induced T_C enhancement could be interpreted as resulting from melt of the super-lattice structure. Furthermore, a possibility of lattice instability around ($\zeta \approx 0.5$) reinforcing the superconductivity should be examined in the high- T_C phase.

References

- [1] Y. Mizuguchi, S. Demura, K. Deguchi, Y. Takano, H. Fujihisa, Y. Gotoh, H. Izawa, and O. Miura, *J. Phys. Soc. Jpn.* **81**, 114725 (2012).
- [2] D. Yazici, I. Jeon, B. D. White, and M. B. Maple, *Physica C* **514**, 218 (2015).
- [3] Y. Mizuguchi, *J. Phys. Chem. Solids* **84**, 32 (2015).
- [4] H. Usui, and K. Kuroki, *Nov. Supercond. Mater.* **1**, 50–63 (2015).
- [5] K. Deguchi, Y. Mizuguchi, S. Demura, H. Hara, T. Watanabe, S. J. Denholme, M. Fujioka, H. Okazaki, T. Ozaki, H. Takeya, T. Yamaguchi, O. Miura, Y. Takano, *Europhys. Lett.* **101**, 1700412 (2013).
- [6] D. Yazici, K. Huang, B. D. White, A. H. Chang, A. J. Friedman, and M. B. Maple, *Philos. Mag.* **93**, 673–680 (2013).
- [7] J. Xing, S. Li, X. Ding, H. Yang, and H. Wen, *Phys. Rev. B* **86**, 214518 (2012).
- [8] S. Demura, Y. Mizuguchi, K. Deguchi, H. Okazaki, H. Hara, T. Watanabe, S. J. Denholme, M. Fujioka, T. Ozaki, H. Fujihisa, Y. Gotoh, O. Miura, T. Yamaguchi, H. Takeya, and Y. Takano, *J. Phys. Soc. Jpn.* **82**, 033708 (2013).
- [9] H. Kotegawa, Y. Tomita, H. Tou, H. Izawa, Y. Mizuguchi, O. Miura, S. Demura, K. Deguchi, and Y. Takano, *J. Phys. Soc. Jpn.* **81**, 103702 (2012).
- [10] C. T. Wolowiec, B. D. White, I. Jeon, D. Yazici, K. Huang, and M. B. Maple, *J. Phys.: Condens. Matter* **25**, 422201 (2013).
- [11] C. T. Wolowiec, D. Yazici, B. D. White, K. Huang, and M. B. Maple, *Phys. Rev. B* **88**, 064503 (2013).
- [12] T. Tomita, M. Ebata, H. Soeda, H. Takahashi, H. Fujihisa, Y. Gotoh, Y. Mizuguchi, H. Izawa, O. Miura, S. Demura, K. Deguchi, and Y. Takano, *J. Phys. Soc. Jpn.* **83**, 063704 (2014).
- [13] R. Sagayama, H. Sagayama, R. Kumai, Y. Murakami, T. Asano, J. Kajitani, R. Higashinaka, T. D. Matsuda, and Y. Aoki, *J. Phys. Soc. Jpn.* **84**, 123703 (2015).
- [14] T. Yildirim, *Phys. Rev. B* **87**, 020506 (2013).
- [15] J. Kajitani, R. Sagayama, H. Sagayama, R. Kumai, Y. Murakami, K. Matsuura, M. Mita, T. Asano, R. Higashinaka, T. D. Matsuda, and Y. Aoki, submitted.
- [16] X. Wan, H.-C. Ding, S. Y. Savrasov, and C.-G. Duan, *Phys. Rev. B* **87**, 115124 (2013).
- [17] B. Li, Z. W. Xing, and G. Q. Huang, *Europhys. Lett.* **101**, 47002 (2013).